

Supporting information for:

Hierarchical Assembly of Homochiral Triple Concentric Helical System in a Novel 3D Supramolecular Metal-organic Framework: Synthesis, Crystal Structure, and SHG Properties

Xiao-Li Sun,^a Wen-Chao Song,^a Shuang-Quan Zang,^{a*} Chen-Xia Du,^a Hong-Wei Hou,^a and Thomas. C. W. Mak^{a,b}

^aDepartment of Chemistry, Zhengzhou University, Zhengzhou 450001, P. R. China

^bDepartment of Chemistry and Center of Novel Functional Molecules, The Chinese University of Hong Kong, Shatin, New Territories, Hong Kong SAR, People's Republic of China

Author for correspondence: Dr. S.-Q. Zang,

E-mail: zangsqzg@zzu.edu.cn

Fax: (+86) 371– 6778 0136

This PDF file includes:

- 1. Experimental Section.**
- 2. Table S1.** Selected bond lengths (Å) and angles(°) of complex **1**.
- 3. Table S2.** Geometrical parameters of hydrogen bonds in complex **1** (in Å and deg).
- 4. Fig. S1.** A view of the coordination environment at the Cd^{II} center in complex **1**.
- 5. Fig. S2.** The side view of the (Cd–DPA)_n chain stabilized by the formation of hydrogen bonds.
- 6. Fig. S3.** The side and top view of the (Cd–bix)_n helical chain(helix **A**).
- 7. Fig. S4.** 3D framework of **1** with triple concentric helical system (Helix **A**, **B**, **C** marked as cyan, pink, green, respectively).
- 8. Fig. S5.** (a) Triple concentric helical system in complex **1** viewed down the *c* axis. (b) Scheme representation of 3D supramolecular framework for **1**.
- 9. Fig. S6.** Side (a) and top (b) view of the (DPA²⁻)_n helical chain (helix **B**) generated through the formation of hydrogen bonding (C10–H10...O5, C10...O5 3.379(1) Å). Symmetry code: A: $x - y, x, z + 1/6$.
- 10. Fig. S7.** Top (a) and side (b) view of the hexagonal arrangement of the helix **A** and **B** in complex **1**. (c) Linkage between the helix **A** and **B**.
- 11. Fig. S8.** The top (a) and side (b) view of the hexagonal arrangement of the helix **B** and **C** in complex **1**. (c) Hydrogen bonding between the helix **B** and **C**. Symmetry code: A: $x - y, x, z + 1/6$.
- 12. Fig. S9.** TG curve for complex **1**.
- 13. Fig. S10.** PXRD pattern of the single crystal of complex **1** under different conditions.

14. Fig. S11. Solid-state emission spectrum of H₂DPA ligand and complex **1**.

15. Reference.

Experimental Section.

(a) The ligand H₂DPA was commercially available chemicals from hhchemistry of China, and the auxiliary ligand bix was synthesized according to the procedure reported by B. F. Abrahams et al.¹

(b) Single-crystal data of complexes were collected on a Bruker SMART APEX CCD diffractometer² with MoK α radiation ($\lambda = 0.71073 \text{ \AA}$) using the ω scan mode at room temperature. Empirical absorption corrections were applied to the intensities using the SADABS program.³ The structures were solved using the program SHELXS-97⁴ and refined with the program SHELXL-97.⁵ All nonhydrogen atoms were subjected to anisotropic refinement. The hydrogen atoms of the organic ligands were included in the structure factor calculation at idealized positions using a riding model and refined isotropically. Possible hydrogen atoms of the coordinated and solvent water molecules were located from difference Fourier maps, and then initially refined making use of SHELXL DFIX restraints. In the final rounds of refinements these H atoms were then placed in fixed positions with assigned isotropic parameters and allowed for as riding atoms.

(c) The second-order nonlinear optical intensity was approximately estimated by measuring a powder sample of 80–150 μm diameter in the form of a pellet relative to urea. A pulsed Q-switched Nd:YAG laser at a wavelength of 1064 nm was used to generate a SHG signal from powder samples. The backscattered SHG light was collected by a spherical concave mirror and passed through a filter that transmits only 532 nm radiation.⁶

Table S1. Selected bond lengths (Å) and angles(°) of complex **1**.

Complex 1			
Cd(1)–N(1)	2.224(5)	O(1)–Cd(1)–O(2)	54.34(16)
Cd(1)–N(4A)	2.236(5)	O(4B)–Cd(1)–O(2)	153.83(14)
Cd(1)–O(1)	2.296(6)	O(3B)–Cd(1)–O(2)	132.17(14)
Cd(1)–O(4B)	2.323(4)	O(1)–Cd(1)–O(4B)	102.65(16)
Cd(1)–O(3B)	2.446(4)	O(1)–Cd(1)–O(3B)	96.95(16)
Cd(1)–O(2)	2.479(4)	O(4B)–Cd(1)–O(3B)	55.06(14)
		N(1)–Cd(1)–O(1)	124.47(19)
		N(1)–Cd(1)–O(2)	82.87(17)
		N(1)–Cd(1)–O(3B)	86.75(16)
		N(1)–Cd(1)–O(4B)	123.15(17)
		N(4A)–Cd(1)–O(4B)	90.95(16)
		N(4A)–Cd(1)–O(1)	109.27(18)
		N(4A)–Cd(1)–O(3B)	141.37(16)
		N(4A)–Cd(1)–O(2)	86.46(16)
		N(1)–Cd(1)–N(4A)	100.26(18)

Symmetry codes: A: $x - y, x, z + 1/6$; B: $-x + 1, -y + 1, z - 1/2$.

Table S2. Geometrical parameters of hydrogen bonds in complex **1** (in Å and deg).

D–H···A	d(D···A)	<DHA
O(1W)–H(1WB)···O(4)	2.941(7)	179.6
O(1W)–H(1WA)···O(2)	3.023(7)	126.4
O(2W)–H(2WA)···O(5)	2.632(18)	177.2
O(2W)–H(2WB)···O(2W) ^a	3.177(15)	178.4
O(3W)–H(3WB)···O(2W) ^b	3.00(8)	178.5
O(3W)–H(3WA)···O(3W) ^c	2.24(3)	123.4
C(10)–H(10)···O(5)	3.394(4)	132.2

Symmetry codes: ^a $y, -x - y, z - 1/6$; ^b $x + 1, y, z$; ^c $x - y, x - 1, z + 1/6$.

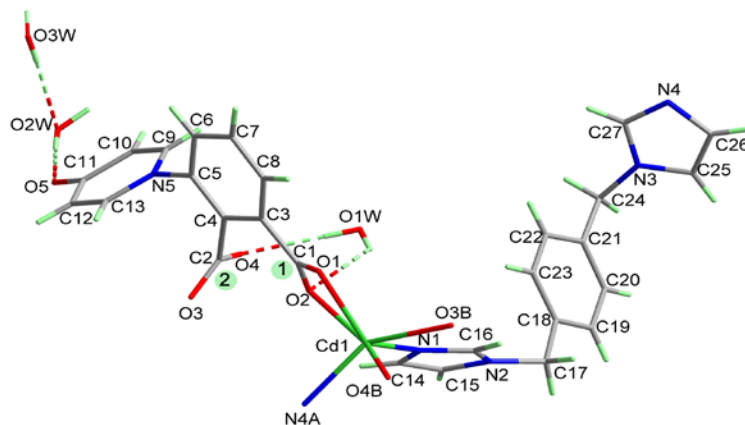


Fig. S1 A view of the coordination environment at the Cd^{II} center in complex **1**. Symmetry codes: A: $x - y, x, z + 1/6$; B: $-x + 1, -1 + y, z - 1/6$.

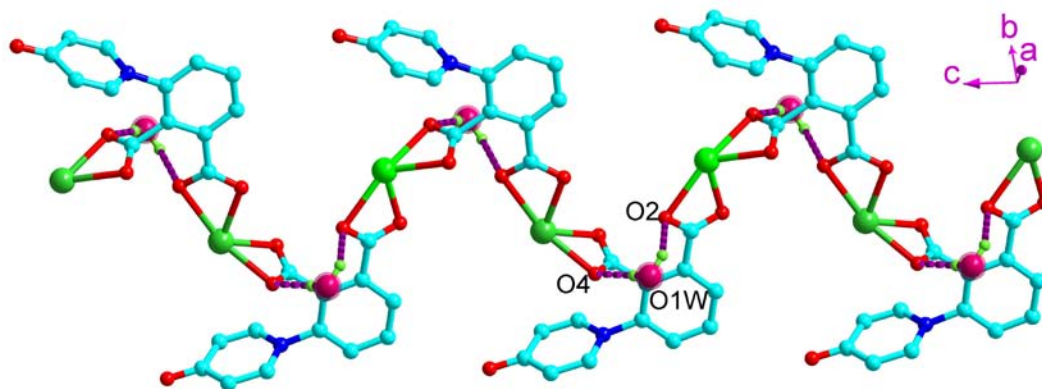


Fig. S2 The side view of the (Cd–DPA)_n chain stabilized by the formation of hydrogen bonds [O1W–H1WA···O2 (O1W···O2 3.023(7) Å) and O1W–H1WB···O4B (O1W···O4B 2.941(7) Å)].

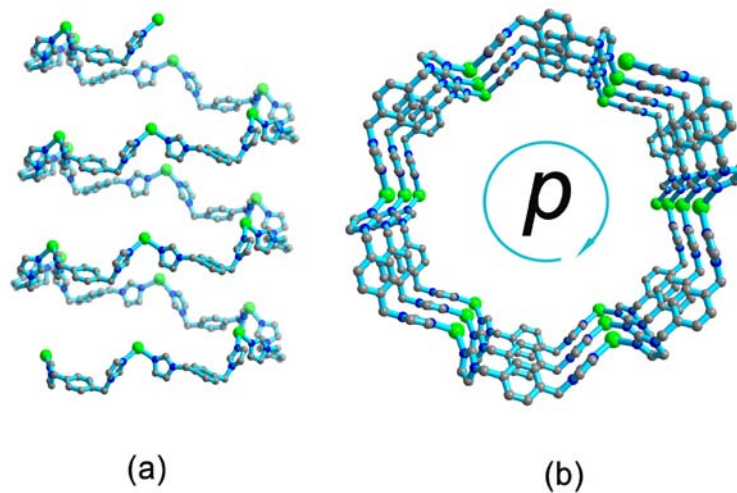


Fig. S3 The side (a) and top view (b) of the $(\text{Cd-bix})_n$ helical chain with right-handed chirality.

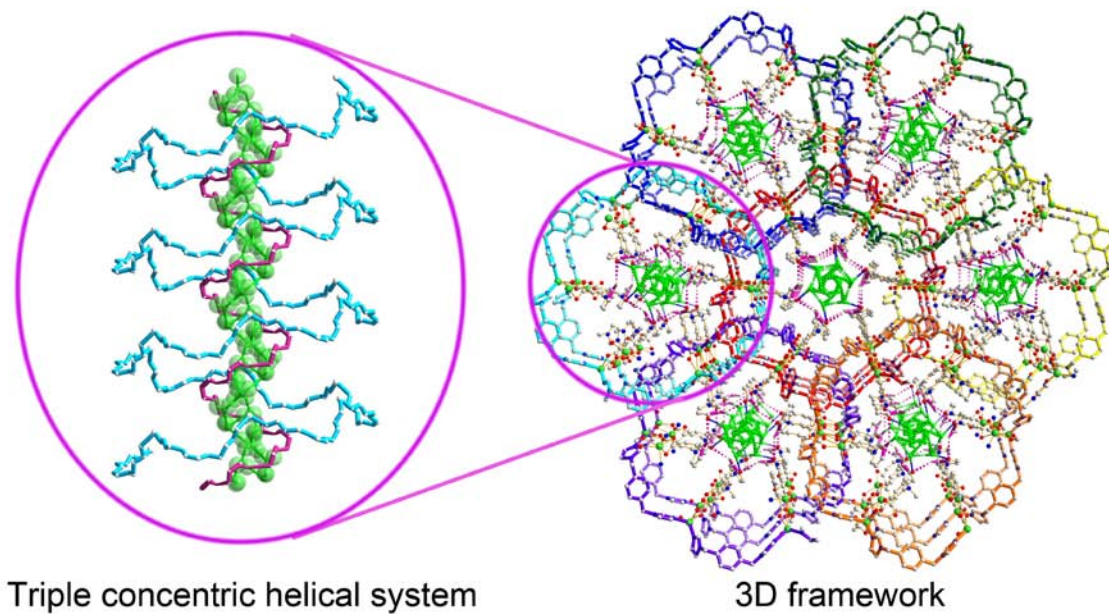


Fig. S4 3D framework of **1** with triple concentric helical system viewed down the c axis (Helix A, B, C marked as cyan, pink, green, respectively.) and.

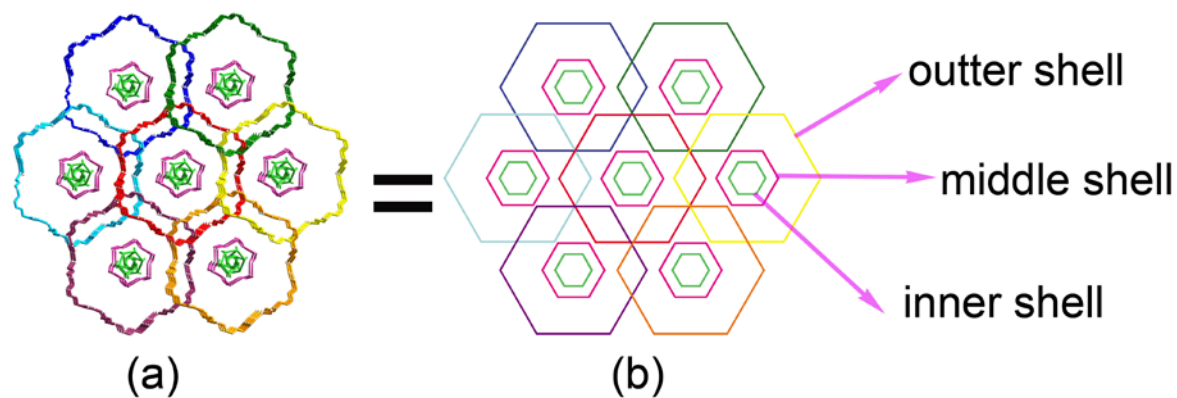


Fig. S5 (a) Triple concentric helical system in complex **1** viewed down the *c* axis. (b) Scheme representation of 3D supramolecular framework for **1**.

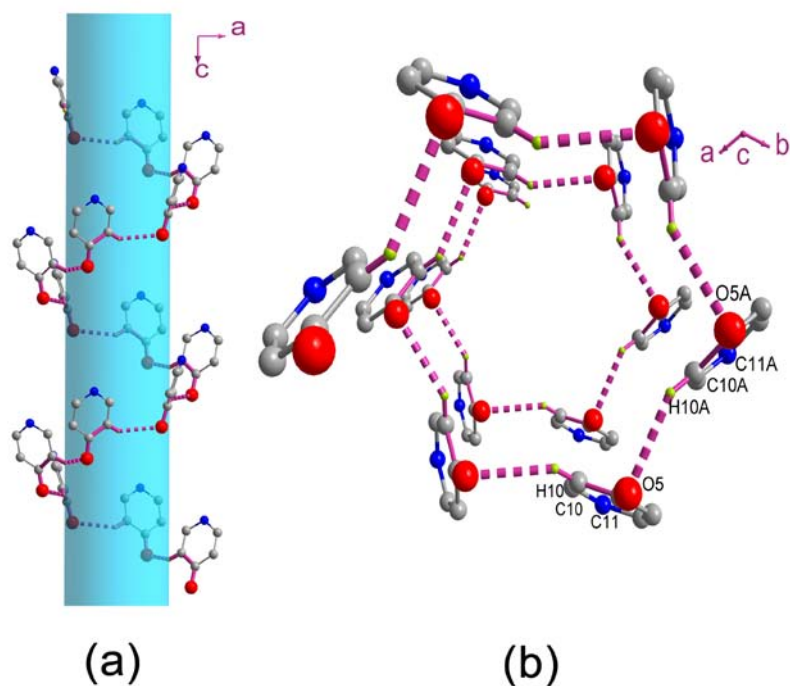


Fig. S6 The side (a) and top (b) view of the $(DPA^{2-})_n$ helical chain (helix **B**) generated through the formation of hydrogen bonding (C10–H10...O5, C10...O5 3.379(1) Å). Symmetry code: A: $x - y, x, z + 1/6$.

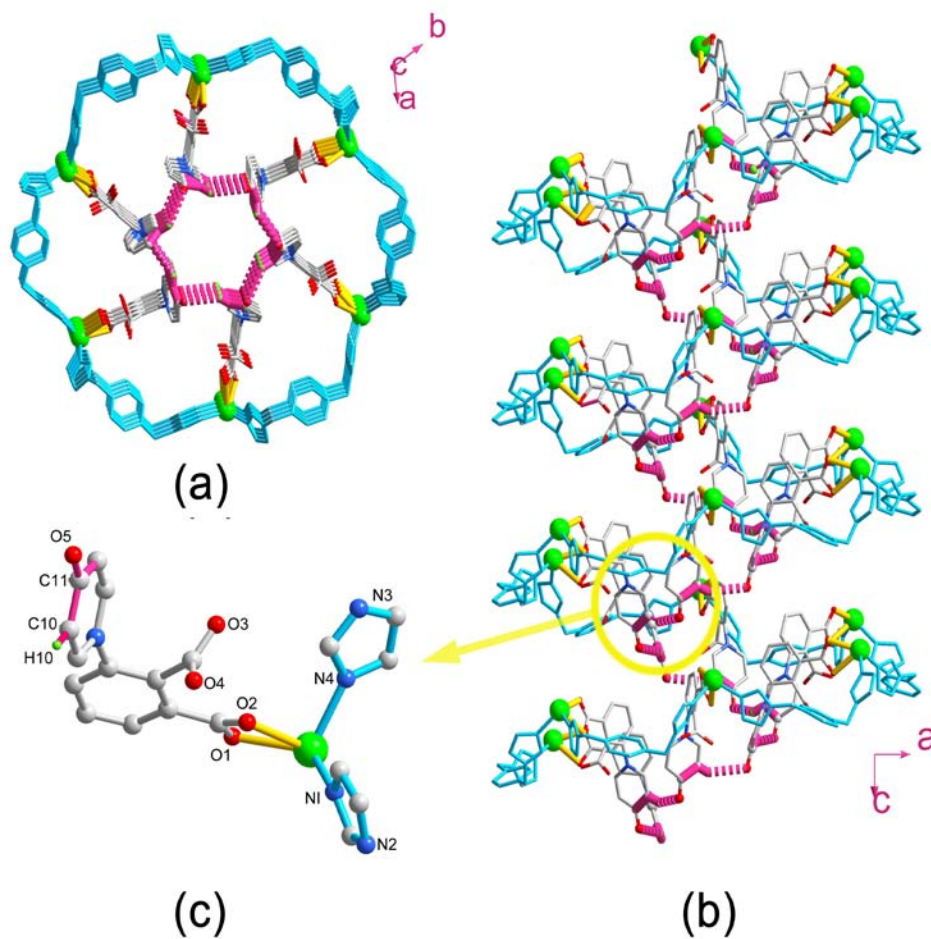


Fig. S7 The top (a) and side (b) view of the hexagonal arrangement of the helix **A** and **B** in complex **1**. (c) Linkage between the helix **A** and **B**.

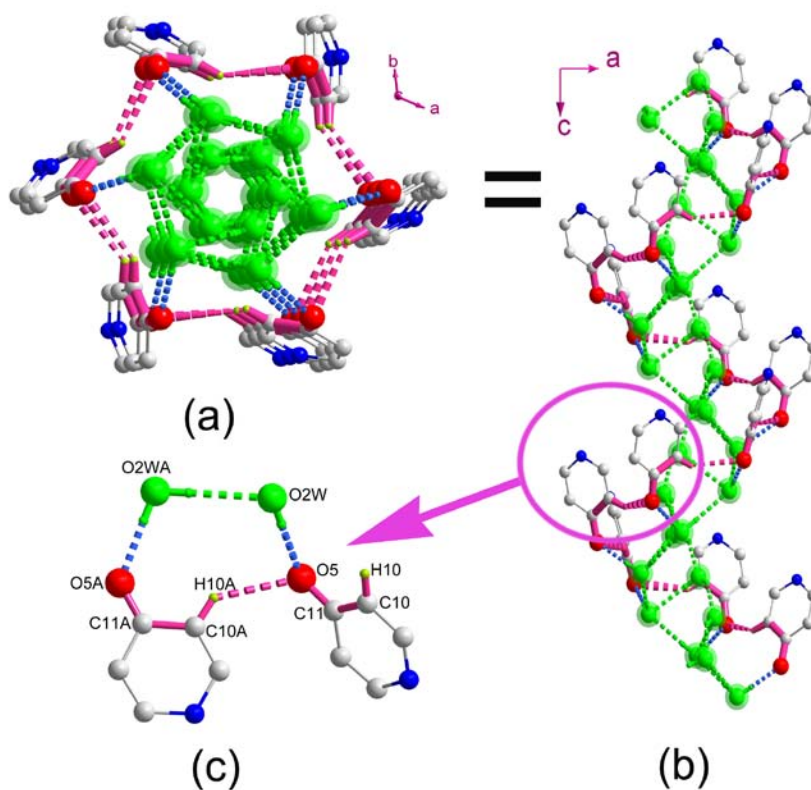


Fig. S8 The top (a) and side (b) view of the hexagonal arrangement of the helix **B** and **C** in complex **1**. (c) Hydrogen bonding between the helix **B** and **C**. Symmetry code: A: $x - y, x, z + 1/6$.

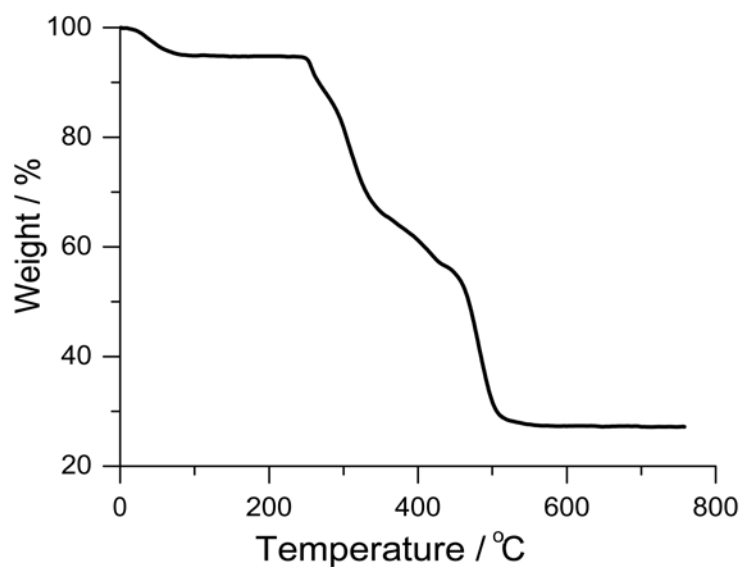


Fig. S9 TG curve for complex **1**.

The first stage involves a 4.95% (calcd, 4.93%) loss in the range of 30–110 °C, which is owing to the weight loss of solvent waters in the porous ($1.75\text{H}_2\text{O}$ for one Cd atom). The abrupt weights lose of coordination waters at approximately 280 °C due to the subsequent decompose of the sample. This is reasonable, since the coordination waters play an indispensable role in the formation of framework.

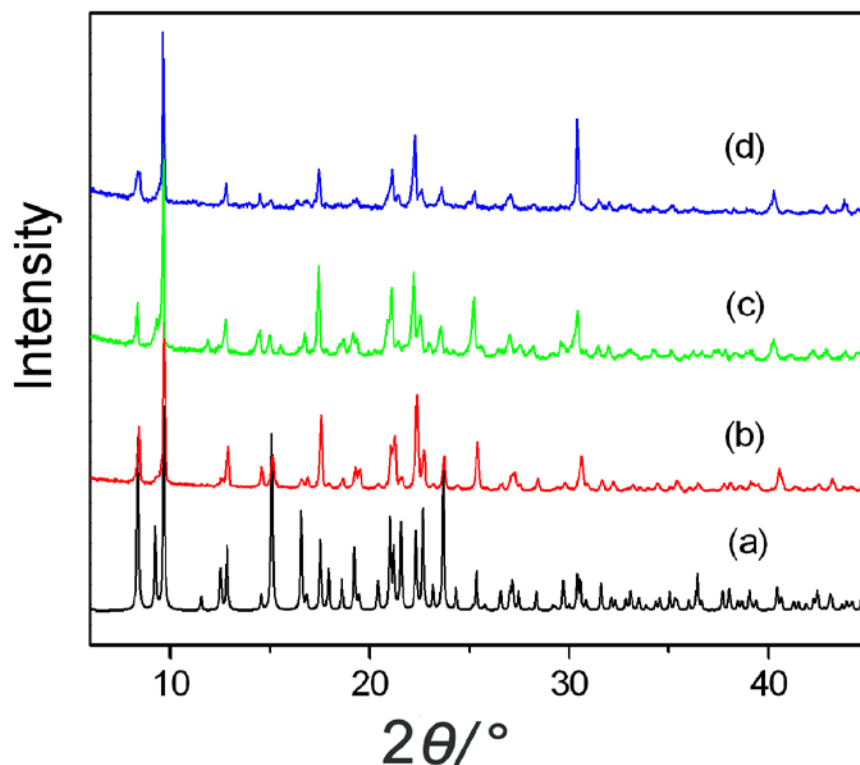


Fig. S10 PXRD pattern of the single crystal of complex **1** under different conditions. (a) PXRD patterns simulated from the single crystal data. (b) PXRD data of complex **1** which collected at room temperature. (c) Sample of **1** dried at 110°C under reduced pressure for 12 h. (d) H₂O immersed sample of **1** after drying.

The positions of the diffraction peaks of the experimental and simulated PXRD patterns matched well, indicating phase purity of the synthesized complex **1**. Powder X-ray diffractograms of the complex **1** before and after expulsion of solvent waters at about 110 °C, the similar spectra of them suggesting the crystalline the integrity of the host lattice is robust to the exclusion of solvent waters. When exposed the dehydrated sample in the water again after 24h which reveals only minor differences in the diffraction patterns and intensities, which suggests the potential reversible adsorbent materials of water molecules. Detailed physical studies about this and several relative interesting frameworks built from the ligand of H₂DPA and bix are in process and will be reported as a full paper.

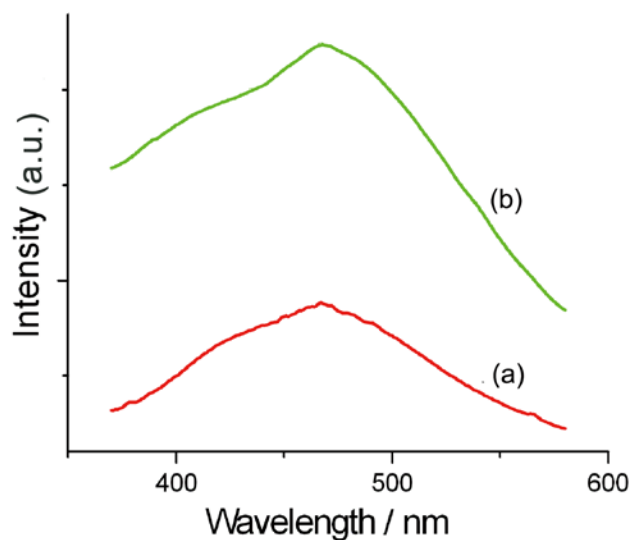


Fig. S11 Fluorescence spectra for H₂DPA ligand (red line) and **1** (green line) at room temperature are shown.

- 1 B. F. Abrahams, B. F. Hoskins, R. Robson and D. A. Slizys, *Acta Crystallogr.* 1998, **C54**, 1666.
- 2 SMART and SAINT. *Area Detector Control and Integration Software*; Siemens Analytical X-Ray Systems, Inc.: Madison, WI, 1996.
- 3 G. M. Sheldrick, *SADABS 2.05*, University of Göttingen, Germany.
- 4 G. M. Sheldrick, *Acta Crystallogr., Sect. A: Found. Crystallogr.*, 1990, **46**, 457; G. M. Sheldrick, *SHELXS-97, Program for solution of crystal structures*, University of Göttingen, Germany, 1997.
- 5 G. M. Sheldrick, *Acta Crystallogr., Sect. A: Found. Crystallogr.*, 2008, **64**, 112.
- 6 R.-G. Xiong, X. Xue, H. Zhao, B. F. Abrahams, X.-Z. You and Z. Xue, *Angew. Chem., Int. Ed.*, 2002, **41**, 3800.